Appl. Sci. **2015**, *5*, 1016-1032; doi:10.3390/app5041016

OPEN ACCESS

applied sciences

ISSN 2076-3417

www.mdpi.com/journal/applsci

Article

The Effects of Cu-doped TiO_2 Thin Films on Hyperplasia, Inflammation and Bacteria Infection

Linhua Li, Ying Xu, Zhi Zhou, Jiang Chen, Ping Yang *, Youhe Yang, Jing'an Li * and Nan Huang

Key Laboratory for Advanced Technologsies of Materials, Ministry of Education, School of Material Science and Engineering, Southwest Jiaotong University, Chengdu 610031, China;
E-Mails: linhua_li@sina.com (L.L.); xying1226@163.com (Y.X.); zhi_zhou123@sina.com (Z.Z.); megane.student@sina.com (J.C.); kesrt@sina.com (Y.Y.); huangnan1956@163.com (N.H.)

* Authors to whom correspondence should be addressed; E-Mails: yangping8@263.net (P.Y.); lijingan@home.swjtu.edu.cn (J.L.); Tel.: +86-28-8763-4148-802 (P.Y.); Fax: +86-28-8760-0625 (P.Y.).

Academic Editor: Hidenori Otsuka

Received: 10 September 2015 / Accepted: 21 October 2015 / Published: 3 November 2015

Abstract: In the present work, different concentrations of Cu ion (1, 2, 5 and 10 wt %) were doped in the TiO_2 film by a sol-gel method and dip coating process. The morphology of the Cu-doped TiO_2 films were characterized by scanning electron microscopy (SEM) and the results showed that the doped Cu made no change to the TiO_2 films. The nitric oxide (NO) release experiment showed that these Cu-doped surfaces showed the ability of catalytic decomposition of exogenous donor *S*-nitroso-*N*-acetyl-penicillamine (SNAP) to generate (NO). Based on fluorescence analysis and CCK-8 quantitative results, such films had the ability to inhibit smooth muscle cells adhesion, proliferation and migration with SNAP *in vitro*. The macrophage adhesion assay and anti-bacterial test proved that such Cu-doped TiO_2 films also possessed anti-inflammatory and anti-bacterial abilities. All the abilities above showed positive correlation with the amounts of the doped Cu. This study suggested that the Cu-doped TiO_2 films were capable of generating physiological levels of NO in the presence of endogenous donor *S*-nitrosothiols (RSNO), endowing the TiO_2 films with anti-hyperplasia, anti-inflammatory and anti-bacterial abilities.

Keywords: Cu-doped; TiO_2 thin film; nitric oxide; biocompatibility

1. Introduction

The principal requirement for cardiovascular implanted materials is biocompatibility, and a genuinely biocompatible cardiovascular implanted material should perform its functions with good anti-coagulation, anti-hyperplasia and anti-inflammation abilities, simultaneously [1,2]. A cardiovascular implanted device, such as a stent, with excellent biocompatibility, will contribute better clinical efficacy to cardiovascular disease and its complications [3,4]. Restenosis and thrombosis are the major complications for stent implantation [5,6]. Thrombosis is mainly due to fibrinogen activation and denaturation, causing a series of subsequent reactions (e.g., activation of platelets and envelope of red blood cell) after implantation [7]. Restenosis is caused by the proliferation and migration of vascular smooth muscle cells (VSMCs) in the vessel wall in response to acute vessel wall injury induced by angioplasty [8]. The application of drug-eluting stent (DES) systems has revolutionized coronary intervention therapy benefiting from their ability to dramatically reduce the possibility of in-stent restenosis through blunting VSMC proliferation [9,10]. However, the results from certain recent meta analyses indicate that drug-eluting coatings result in the subsequent serious complication of late angiographic stent thrombosis (LAST), suggesting insufficient function in inhibiting the excessive proliferation and migration of the VSMCs [11,12]. So, enhancing the function of inhibiting VSMCs becomes a problem which urgently needs to be resolved for the cardiovascular stent. Lots of clinical cases have proved that inflammation and bacterial infections also should be considered during vascular stent implantation [13,14]. Compelling evidence for the importance of inflammation and atherosclerosis at both the basic and clinical level has evolved in parallel. Inflammation involved in the various stages of atherosclerosis—from initiation, through progression, and ultimately, the thrombotic complications of atherosclerosis [15,16]. Moreover, a certain therapeutic has been shown to reduce coronary heart disease and limit the inflammation treatment [17]. In addition, bacterial composition on the implant materials may cause of peri-implantitis, which will influence the success and survival rates of implant materials [18,19]. Therefore, antibacterial efficacy must be considered during medical devices' implantation.

Titanium dioxide (TiO_2) has been widely used in terms of electronics, optics and medicine for its unique optical, electrical and chemical properties [20]. In recent years, TiO_2 has attracted wide attention for its potential application in cardiovascular implanted biomaterials [21,22]. Several studies have demonstrated that the TiO_2 film possesses excellent blood compatibility and cell compatibility while its anti-hyperplasia and anti-inflammation functions need further improvement [23,24]. In the meantime, the applications of TiO_2 films doped by nanostructures in antibacterial purposes, cell growth and differentiation have been recently reported [25–27]. The physiological vascular endothelial layer inspired surface functionalization provides a good choice to solve this problem. Nitric oxide (NO) produced by healthy endothelial tissue is the most important functional molecules on anti-hyperplasia and anti-inflammation of the cardiovascular system [28,29]. Furthermore, lots of researches have proved that NO donating materials surfaces can significantly improve their functions of anti-coagulant, anti-hyperplasia, preventing microbial growth [30] and enhancing wound healing [31–33]. In order to overcome the storage limitation of NO donating materials surfaces, a potentially NO generating material would be used to enhance the biocompatibility of the implanted devices. It is well known that Cu(II)/Cu(I) ions can catalytically decomposes endogenous S-nitrosothiols (RSNO) to release NO *in vivo* [34–38]. Hence, it should be possible to utilize endogenous reducing equivalents (e.g., ascorbate,

L-glutathione (GSH), and cysteine (CySH)) and the endogenous NO precursors (e.g., *S*-nitrosoglutathione (GSNO), *S*-nitrosocysteine (CysNO), and *S*-nitrosoalbumin (Alb-SNO) in blood to generate locally enhanced NO levels at the biomaterials–blood interface by immobilizing catalytic Cu(II)/Cu(I) sites [39]. So, TiO_2 films doped with Cu have been suggested to have better blood and cell compatibility, and anti-hyperplasia and anti-inflammation functions, simultaneously. Our recent studies showed that Cu-doped TiO_2 thin films could effectively suppress platelet adhesion, activation and aggregation [39], while the Cu-doped TiO_2 films' capability of anti-hyperplasia and anti-inflammation was not reported, and the anti-bacterial property of the Cu-doped TiO_2 films was not investigated.

In this work, we prepared the Cu-doped TiO_2 films by sol-gel method because sol-gel method for preparing film has many advantages unmatched by other methods, such as the use of simple equipment, achieving film formation at normal temperature, quantitative doping, and effective control of the film composition and microstructure [23,39]. As described in previous work, different concentrations of Cu were doped into the TiO_2 films [39], but the Cu-induced catalytic activity films could not *in situ* induce NO releasing without donor; therefore, *S*-nitroso-*N*-acetyl-penicillamine (SNAP) must participate in the cell compatibility tests and NO release detection since exogenous SNAP would decompose to release NO in the presence of catalytic agents. The influences of Cu addition and concentrations on the surface morphology were characterized by scanning electron microscopy (SEM), and the anti-hyperplasia, anti-inflammation and anti-bacterial functions of the films were also investigated, respectively.

2. Experimental Section

2.1. Materials and Reagents

Ethanol (C_2H_5OH), tetrabutyltitanate ($Ti(OC_4H_9)_4$), aceticacid (CH_3COOH), acetylacetone ($C_5H_8O_2$), cupric nitrate trihydrate ($Cu(NO_3)_2 \cdot 3H_2O$) and Silicon (Wafer100) wafers were purchased from Sigma-Aldrich, and used as received. *S*-nitroso-*N*-acetyl-pencillamine (SNAP), L-glutathione (GSH) and Griess reagent were all purchased from Sigma-Aldrich Chemical Co. (St. Louis, MO, USA) Ultra-pure water (>18.0 mΩ) was used in the NO releasing experiment. F12 culture medium and rhodamine staining reagent were purchased from BD Biosciences, San Jose, CA, USA.

2.2. Cu-doped TiO_2 Thin Films Preparation

Cu-doped TiO_2 thin films with different Cu concentrations were prepared as described in the previous work [39]. At first, silicon wafers were cut into small plates (7 mm × 7 mm) and sequentially cleaned in acetone, alcohol, and distilled water (dH_2O) ultrasonically for 10 min three times, respectively. Subsequently, $Ti(OC_4H_9)_4$ was added to the mixture of ethanol and acetic acid under vigorous stirring to form a solution. The ratio of each reagent was $Ti(OC_4H_9)_4$:C_2H_5OH:CH_3COOH:$C_5H_8O_2$ = 9:36:5:1. After this, a certain proportion of $Cu(NO_3)_2 \cdot 3H_2O$ was added to the solution, the molar ratio of Cu and Ti was 1% (labeled as Cu1), 2% (labeled as Cu2), 5% (labeled as Cu3) and 10% (labeled as Cu4), respectively. Then, Cu-doped TiO_2 thin films were deposited on silicon substrates by a dip-coating process at room temperature with the withdrawing speed of 20 mm/min. Dip-coating and preannealing at 100 °C for 10 min were repeated and multilayers of Cu-doped TiO_2 thin films can be obtained. This procedure was operated three times. The total film thickness was estimated to be 130 nm. Finally,

each sample was thermally treated at 450 °C for 1 h. The detailed process of preparation of the Cu-doped TiO_2 thin films was shown in Figure 1.

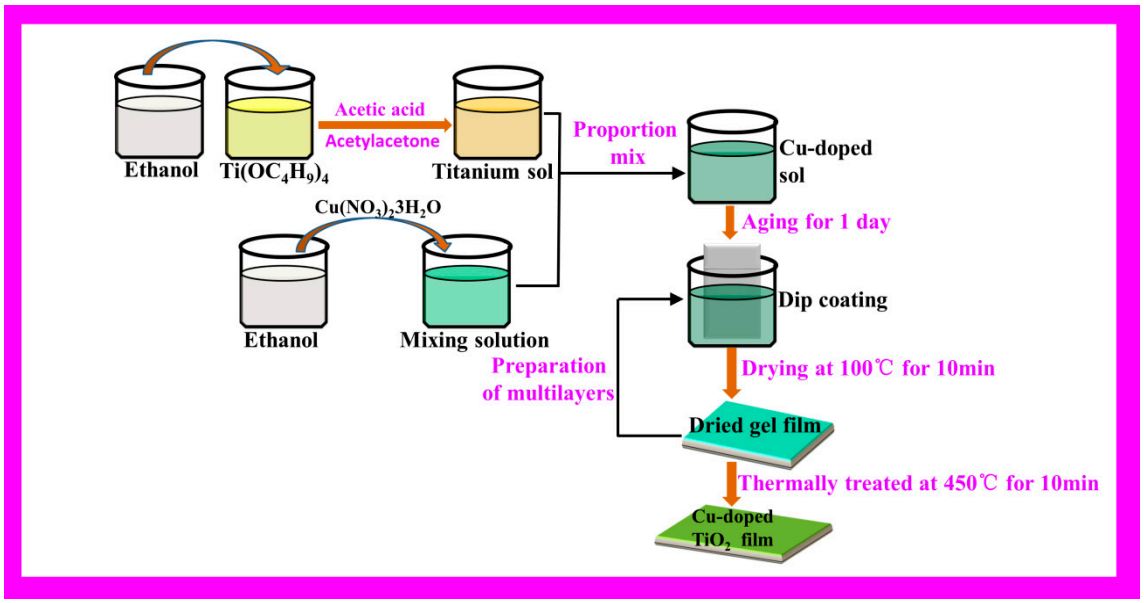

Figure 1. The detailed process of preparation of the Cu-doped TiO_2 thin films.

2.3. Surface Morphology Characterization

The surface morphology and roughness of the Cu-doped TiO_2 thin films were characterized by atomic force microscopy (AFM, JPK Instruments, Berlin, Germany) in tapping mode [40]. The crystalline structure of the Cu doped TiO_2 films were studied by X-ray diffraction (XRD, X' Pert ProMPD, PANalytical B.V., Almelo, The Netherlands) [39]. The amounts of the doped Cu on each TiO_2 samples were measured by a typical micro BCA method [41].

2.4. Nitric Oxide (NO) Release in Vitro

The release of NO catalyzed by Cu-doped TiO_2 thin films was examined using Savillee-Griess reagent [42]. As a stable degradation product of NO, the content of nitrite could represent the release of NO. In short, a 200 μL solution containing 65 μM SNAP and 30 μM GSH were added onto the surface of all the samples (Cu0, Cu1, Cu2, Cu3 and Cu4). Then, SNAP was detected before and after the catalytic decomposition for 1 h, 2 h and 3 h, respectively, by reacting with equal-volume Savillee-Griess reagent, and the absorption was read at 540 nm. The amount of releasing NO was obtained by calculating the decrease of SNAP after catalytic decomposition.

2.5. Isolation and Culture of HUASMC

Human umbilical arterial smooth muscle cells (HUASMCs, Maternal and Child Health Hospital of Chengdu, China) were obtained from neonatal umbilical cord by the traditional method [43]. In brief, the human umbilical cord was thoroughly rinsed with PBS buffer to remove the residual blood. Then, tearing the outer connective tissue and peeling the outer fibroblast layer so the artery was resected from the umbilical cord. Subsequently, the umbilical artery longitudinally broke away, and the ECs inside

were gently scraped by a sharp tweezer. After that, the muscle tissue was sufficiently washed with PBS buffer, and then cut into small pieces. The tissue pieces were seeded into a culture flask, cultured with 5 mL medium F12 containing 0.5 mL FBS, and incubated at 37 °C in a humidified atmosphere containing 95% air and 5% CO_2. The tissue blocks were removed after the HUASMCs migrated to the flask wall. Replicated cultures were performed by trypsinization as cells were approaching confluence. Cells were fed with freshly prepared growth medium every 24 h. The third passage of SMCs with the concentration of 5×10^4 cells/mL was used. HUASMCs derived from new born umbilical vein were approved by the Maternal and Child Health Hospital Institutional Review Board, and none of the research performed violated the Helsinki Declaration [44].

2.6. HUASMC Morphology and Proliferation

A rhodamine staining assay was used for observing the morphology and number of the HUASMC on each samples after cultured for 1 day and 3 days, respectively. The samples cultured with HUASMCs were rinsed with phosphate buffer solution (PBS, pH = 7.4) at 37 °C three times, then fixed with 4% paraformaldehyde for 12 h at room temperature. After a rinsing step, the samples were immunofluorescence stained with rhodamine (70 μM each sample) under dark conditions for 15 min. Washed three times again, the samples were air dried under dark conditions. At last, all samples were observed under a Leica DMRX fluorescence microscope. HUASMC proliferation was investigated by Cell Counting Kit-8 (CCK-8, Boshide, Wuhan, China) after incubation for 1 and 3 days, respectively [45].

2.7. HUASMC Migration

Firstly, the medical titanium foil was cut into a rectangular size of 1 cm × 1 cm. Cleaned by a conventional method, titanium foils were half cover with different concentrations of Cu-doped TiO_2 thin films (Cu0, Cu1, Cu2, Cu3 and Cu4) as the method described above. All the samples were bent at right angles from the middle with tweezers, so that one side of the titanium foils is titanium, the other side is film. Titanium is placed at the bottom to culture cells to obtain a confluent monolayer. Then, HUASMCs were seeded onto samples with a density of 5×10^5 cells/cm^2. After culture for 6 h (the HUASMCs formed a confluent monolayer on this half untreated titanium), the rectangular of specimen was vertically turned over and transferred to a new well plate, and was covered by the new culture medium. All the specimens were cultured for 1 day in an incubator at 37 °C. All the culture experiments above were conducted in sterile conditions. After fluorescence staining as above, the samples were observed by a Leica DMRX fluorescence microscope (Leica, Heidelberg, Baden-Württemberg, Germany).

2.8. Morphology of Macrophages

Peritoneal macrophages derived from the abdominal cavity of Sprague Dawley (SD) rats (Dashuo Co., Ltd., Chengdu, China) were isolated using the following method: SD rats were treated by cervical dislocation, immersed in 75% alcohol for 15 min. Next, the rats were set in supine, fixed extremities and extracted the abdominal wall with tweezers. Cutting a small hole in the skin and injection of 10 mL cell culture medium into its intraperitoneal, and then the abdominal cavity was gently massaged about 5–10 min. The cell culture medium was sucked out from abdominal cavity with a dropper and centrifuged at

1200 rpm for 5 min. The supernatant of the centrifuge tube was discarded, hereafter fresh culture medium containing 10% fetal calf serum was added in the centrifuge tube to dilute the concentration of the cell suspension to 1×10^5 cells/mL. Then, 1 mL of the cells suspension was added onto each sample (Cu0, Cu1, Cu2, Cu3 and Cu4) in 24-well plates and incubated (37 °C, 5% CO_2) for 3 days. All the macrophage culture experiments above were operated in the sterile condition. Thereafter, samples were rinsed for three times with PBS (pH = 7.4), 5 min each time, and fixed in 2.5% glutaraldehyde for 12 h. A rhodamine staining was performed to statistic the number of attached macrophages on each samples directly (15 images each sample), and SEM characterization was performed to observe the morphology of the macrophages on the samples. Before the SEM characterization, samples were dehydrated, dealcoholized, followed with drying by critical point dryer (BAL-TEL CPD 030, Leica, Heidelberg, Baden-Württemberg, Germany), and gold deposited.

2.9. Anti-Bacterial Performance Assay

The anti-bacterial experimental procedure was performed under sterile conditions as follows. Firstly, 0.1 g of different concentrations of copper-doped titanium dioxide sol powder by heat treatment was pressed into tablets with a diameter of 10 mm and a thickness of 2 mm, which contained activated bacteria. Secondly, cryopreserved *E. coli* with inoculation loop was inoculated on agar medium and placed in an incubator at 37 °C, and the third generation activation *E. coli* loop which was incubated at 37 °C for 48 h was added to an erlenmeyer flasks containing PBS buffer (pH = 7.4), and after a mixing operation, bacterial suspension with a concentration of $5 \times l0^6$ cfu/mL was obtained. Then, 0.1 mL of bacterial suspension was added drop wise the surface of solidified beef extract peptone agar until the petri dish was covered completely, and was dried in the room temperature for 5 min. Finally, the prepared samples were placed in the bacterial culture medium surface, and incubated in the incubator 37 °C, bacteriostatic ring was observed after 24 h.

2.10. Statistical Analysis

In this work, all the experiments were replicated thrice ($n = 3$), and all the quantitative results were expressed as mean ± standard deviation (SD). The data were analyzed by the software SPSS 11.5 (Chicago, IL, USA). Statistical significance was accepted at a p-value of less than 0.05 ($p < 0.05$).

3. Results and Discussion

3.1. Surface Characterization

The morphology and roughness of the Cu0, Cu1, Cu2, Cu3 and Cu4 surfaces observed by AFM are shown in Figure 2. It was obvious that Cu0, Cu1 and Cu2 displayed smooth surfaces, with their roughness 0.40 ± 0.03 nm, 0.42 ± 0.02 nm and 0.43 ± 0.03 nm, respectively. Nevertheless, Cu3 and Cu4 samples showed significantly rougher surfaces compared to Cu0, Cu1 and Cu2 (Ra: Cu0, Cu1 and Cu2 < Cu3 < Cu4). The AFM results suggested that a little amount of Cu doped in the TiO_2 could not remarkably change its morphology and roughness, while a large quantity of Cu doped in the TiO_2 could significantly increase its roughness and change its morphology.

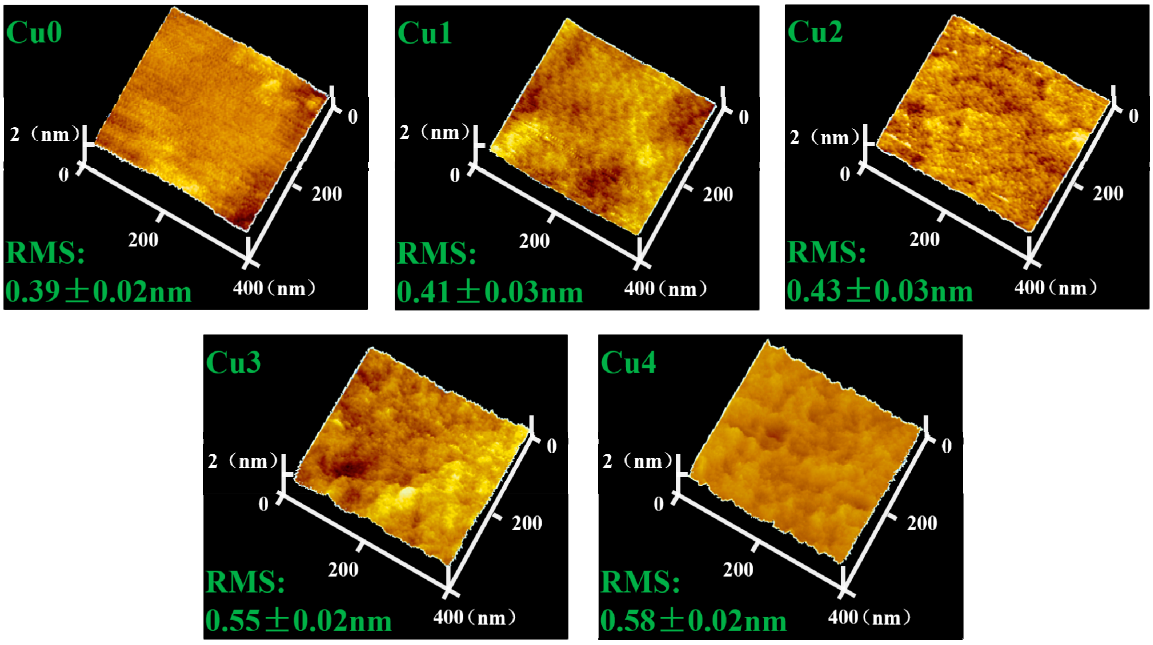

Figure 2. The AFM characterization of the Cu0, Cu1, Cu2, Cu3 and Cu4 samples.

The crystalline structures of the Cu doped TiO_2 films (Cu0, Cu1, Cu2, Cu3 and Cu4) detected by XRD are displayed in Figure 3. The major phase was anatase when the films were calcined at 450 °C. Small diffraction peaks of CuO appear at $2\theta = 35.6°$ on Cu4 samples. No Cu peak was observed on Cu1, Cu2 or Cu3 samples, and it could be attributed to either small amount of Cu loading or very small Cu cluster size. The XRD results indicated that the doped Cu element mainly survived as a state of CuO.

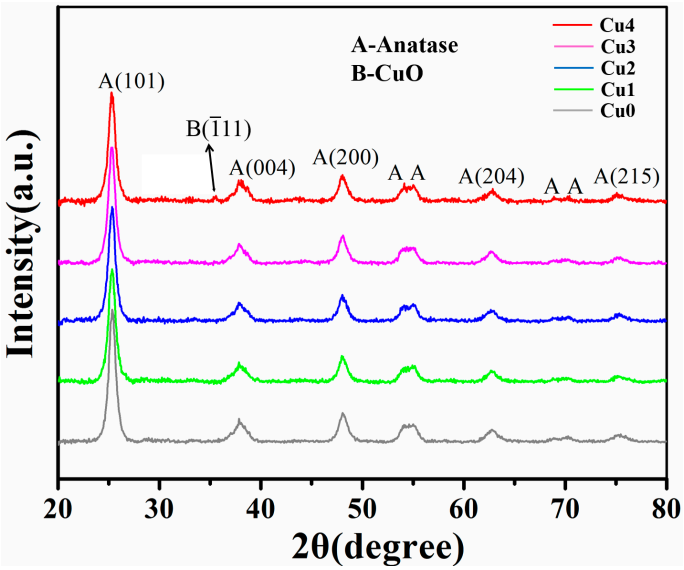

Figure 3. XRD results of the Cu0, Cu1, Cu2, Cu3 and Cu4 samples.

The micro BCA test in Figure 4 shows the amounts of Cu survived in the Cu0, Cu1, Cu2, Cu3 and Cu4. It was clear that the amounts of Cu on the surface increased with the amounts of doped Cu (Cu4 > Cu3 > Cu2 >Cu1, * $p < 0.05$). Cu4 possessed almost three times' the amounts of Cu compared with Cu1 and Cu2, and possessed the most Cu on its surface, which was consistent with the XRD results.

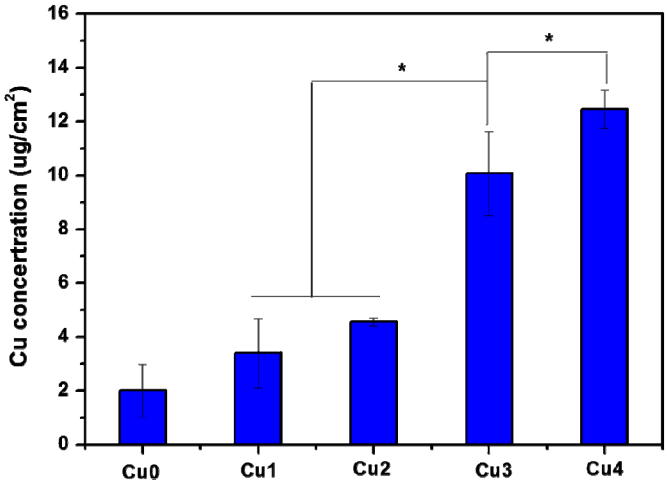

Figure 4. The quantity results of Cu in the Cu0, Cu1, Cu2, Cu3 and Cu4 samples by micro BCA assay (mean ± SD, * $p < 0.05$, $n = 3$).

3.2. Nitric Oxide Release in Vitro

In vitro catalytic degradation of SNAP was performed using Saville-Griessreagent to assess the function of NO release (Figure 5). It could be seen that there was no substantial release of NO from the surface of Cu0, which indicated that TiO_2 itself could not induce the exogenous donor SNAP to produce NO. Obviously, there were significant NO released from the Cu doped TiO_2 samples, and the more Cu doped in the TiO_2 films, the faster NO was released from the samples' surfaces (catalytic generation of NO: Cu4 > Cu3 > Cu2 > Cu1). Notably, the NO generation ratios of Cu2, Cu3 and Cu4 samples were within the range of 0.5×10^{-1} mol/cm^2·min to 4×10^{-1} mol/cm^2·min, which was in the range of NO generation ratios of healthy endothelial cells [39]. The results above indicated that the doped Cu could catalyze SNAP in producing NO, and Cu4 sample which was doped with the most Cu, possessed the fastest NO release ratio.

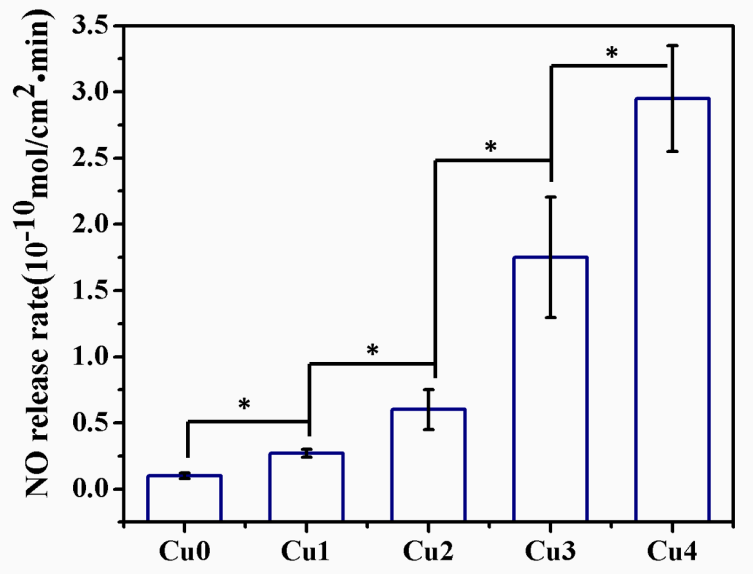

Figure 5. Catalytic generation of NO by Cu0, Cu1, Cu2, Cu3 and Cu4 samples using GSNO as the substrate (mean ± SD, * $p < 0.05$, $n = 3$).

3.3. SMC Attachment and Proliferation

Suppression of vascular smooth muscle cells (SMCs) from excessive proliferation is an effective method for reducing the in-stent restenosis and hyperplasia, which is the most serious clinical problem in the treatment of cardiovascular diseases [46]. Thus, SMCs' attachment and proliferation test *in vitro* can be performed to investigate the anti-hyperplasia property of biomaterials. The fluorescence images of the SMCs on all samples after one day and three days of culturing are presented in Figure 6. It seemed that there were more SMCs on no-donor samples surfaces compared to the donor surface, and the more Cu doped in the TiO_2 films, the less SMCs that were adherent on the samples, suggesting Cu ions may have some influence on the attached number of SMCs. It also could be seen that the SMCs on the no-donor surfaces showed a synthetic phenotype (polygon morphology), while the SMCs on the donor surfaces presented a contractile phenotype (spindle morphology). This result indicated that the Cu-doped surface could promote the SMCs' phenotypic contraction and inhibit SMCs' excessive proliferation by catalyzing donor release NO.

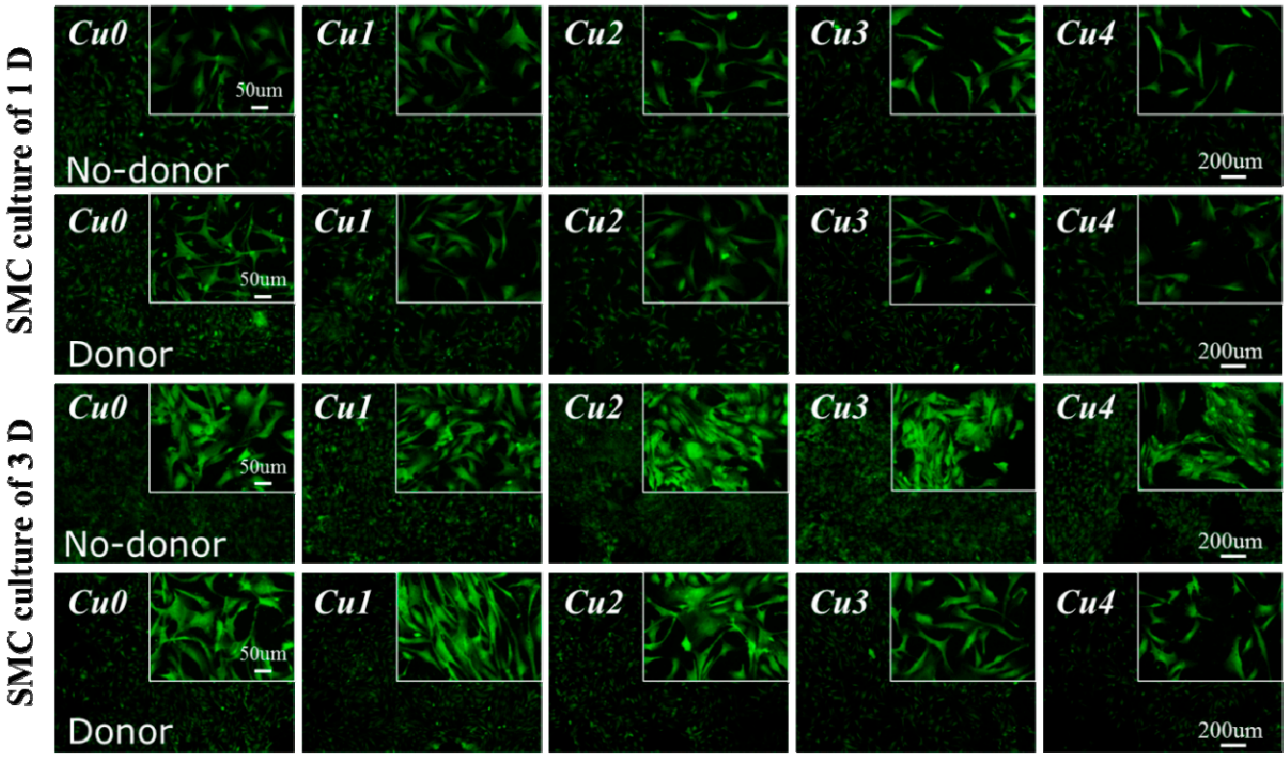

Figure 6. The fluorescence staining of SMC on the Cu0, Cu1, Cu2, Cu3 and Cu4 surfaces after one day and three days of culturing, respectively.

Figure 7 displays the amounts of SMCs on the Cu0, Cu1, Cu2, Cu3 and Cu4 surfaces by CCK-8 assay after one day and three day cultures, respectively. The results showed that increasing doped amounts of Cu in the TiO_2 films (Cu1, Cu2, Cu3 and Cu4) could reduce the attachment of SMCs (attached SMC numbers in one day: Cu4 < Cu3 < Cu2 < Cu1 < Cu0), but could not effectively inhibit the SMCs' proliferation because there were no significant differences between all the no-donor samples and the number of SMCs after three days of culture. Notably, the donor samples showed a significantly lower number of SMC compared with the no-donor samples, and the number of SMCs reduced as the amount

of doped Cu increased. This result was consistent with the NO release result and the SMC staining result, indicating the amount of doped Cu was positively correlated with the released RSNO and was negatively correlated with the SMCs' attachment and proliferation. The results above demonstrated that the Cu-doped TiO_2 films could significantly induce SNAP to release NO and further inhibit SMCs' attachment and proliferation.

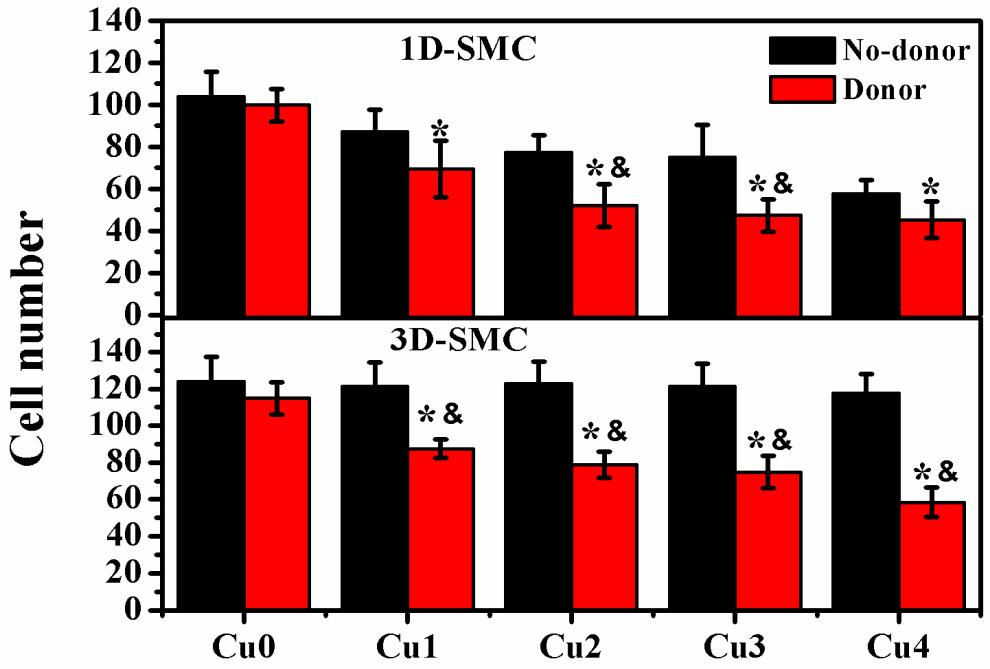

Figure 7. Investigation of SMC number on the Cu0, Cu1, Cu2, Cu3 and Cu4 surfaces *via* CCK-8 assay after cultures of one day and three days, respectively (mean ± SD, * $p < 0.05$ compared with Cu0, $^{\&}$ $p < 0.05$ compared with no-donor samples, $n = 3$).

3.4. HUASMC Migration

It is well known that the proliferation and migration of SMCs on the biomaterials surface could lead to pathological growth of the endothelial cell and further stent restenosis [47]. Therefore, SMC migration tests *in vitro* can be performed as an evaluation of the anti-hyperplasia of the biomaterials. Figure 8 presents the fluorescence images of SMCs' migration on each sample (Cu0, Cu1, Cu2, Cu3 and Cu4). The statistical results show that there are a large number of cultured SMCs migrated on the surface of the no-donor group Cu0, and which had a long migration distance of 1175 ± 25 μm. The doped Cu had a small inhibitory effect on the SMCs' migration, but this effect was not remarkable in the fluorescence images. Notably, the donor group possessed a significant inhibitory effect on the SMCs' migration, and this effect was positively correlated with the amounts of the doped Cu. Accordingly, the Cu4 had the strongest effect in demonstrating SMCs' migration, in which the SMCs only migrated 545 ± 15 μm. This result was consistent with the NO release result and the SMC proliferation result. Thus, the results proved that the Cu doped TiO_2 films with suitable SNAP plays an important role in regulating not only SMCs' proliferation but also their migration.

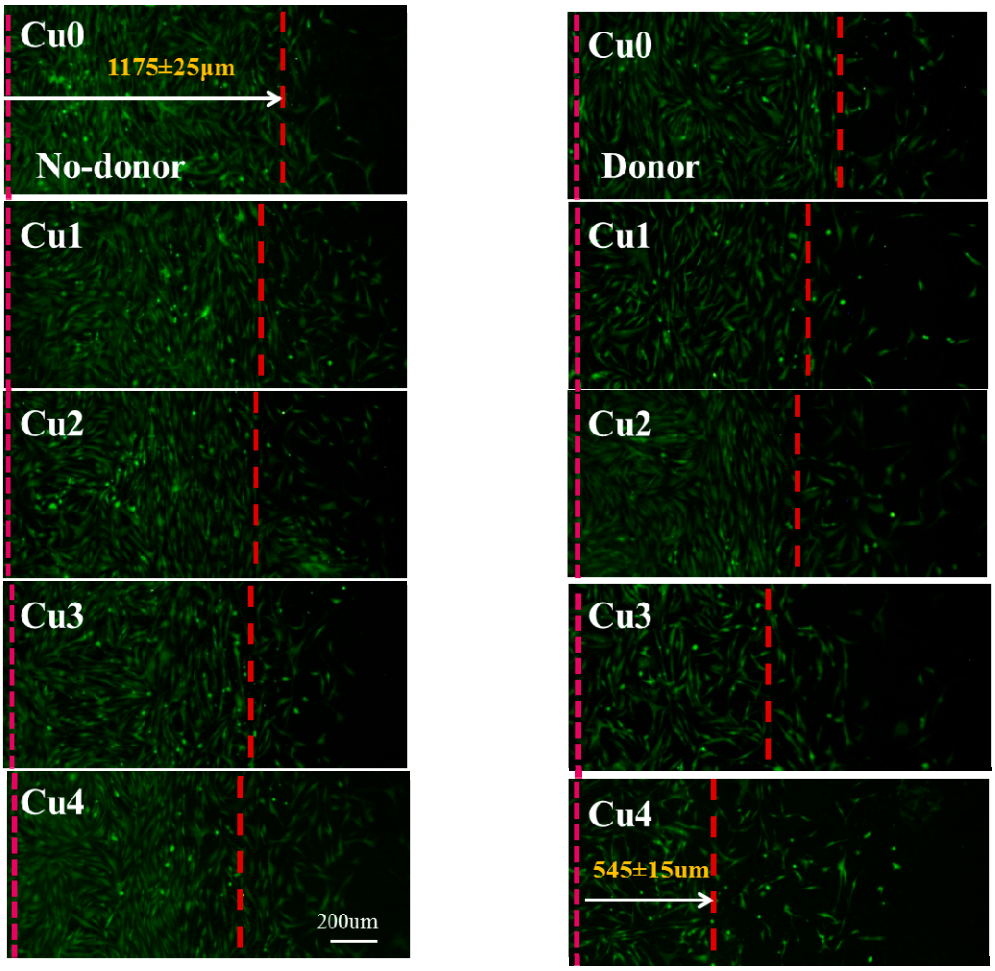

Figure 8. Migration of SMCs on the Cu0, Cu1, Cu2, Cu3 and Cu4 surfaces after culture of one day. The migration distance was calculated from at least 12 images.

3.5. Attachment and Morphology of Macrophages

The attachment and activation of macrophages on a biomaterial's surface could lead to inflammatory response. Therefore, the attachment and activation of macrophages on Cu-doped TiO_2 thin films was performed to evaluate the anti-inflammation function of the film. Figure 9 shows the fluorescence images and counting results of the macrophages on Cu0, Cu1, Cu2, Cu3 and Cu4 surfaces. Obviously, the macrophages on the Cu3 and Cu4 were significantly less than the cells on Cu0, Cu1 and Cu2, and the morphology of macrophages showed typical shrinkage, suggesting a non-activated phenotype. SEM micrographs (Figure 10) displayed further results of the macrophages' morphology. The macrophages on the samples of Cu0, Cu1 and Cu2 showed a multilateral and spreading morphology, with many pseudopods stretching out and aggregating, indicating an activated phenotype, while the macrophages on the Cu3 and Cu4 samples showed a round and shrinking morphology, suggesting a non-activated phenotype. This result demonstrated that the more Cu doped in the TiO_2 films, the fewer macrophages adherent to and activated on the surfaces. The result also suggested that the Cu doped TiO_2 thin film surfaces may be toxic while the human body contains 0.1 g of Cu per 75 kg of body weight and it is widely distributed in the blood, bone and muscle [39].

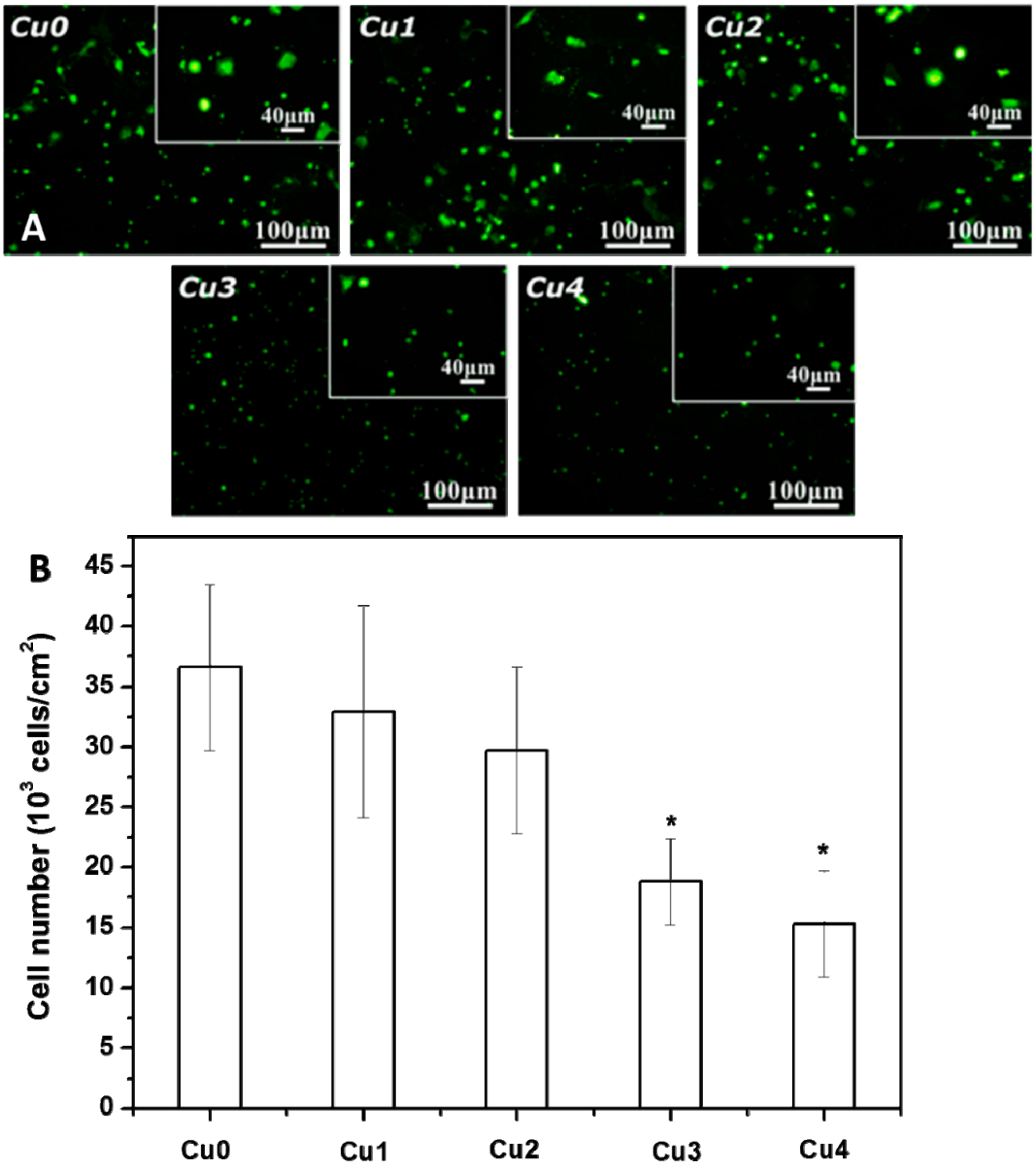

Figure 9. (**A**) The fluorescence photographs and (**B**) cell counting results of macrophages on the Cu0, Cu1, Cu2, Cu3 and Cu4 surfaces after 24 h incubation (mean ± SD, * $p < 0.05$ compared with Cu0, Cu1 and Cu2, $n = 3$).

The change of macrophage morphology often accompanied by their immune functions, such as: phage function and secretion function changes [48]. Activated macrophages can release specific chemical factors, which induce other inflammatory cells and cytokines to flock to the trauma location and cause inflammation. Thus, the attachment and activation of macrophages on the biomaterials is often detected as an evaluation of their anti-inflammation properties. Therefore, the above results showed that the samples Cu3 and Cu4 had good anti-inflammatory properties.

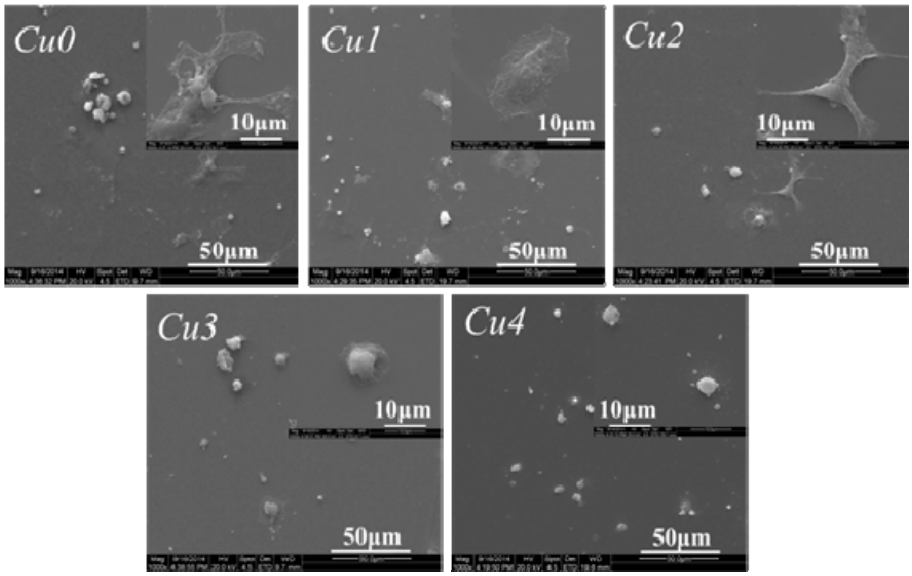

Figure 10. The SEM characterization of macrophages on the Cu0, Cu1, Cu2, Cu3 and Cu4 surfaces after 24 h of incubation.

3.6. Antibacterial Experimental Results

Figure 11 depicts the results of the anti-microbial property on the Cu0, Cu1, Cu2, Cu3 and Cu4 samples. The Cu/TiO_2 2 mm heat treated tablets were fabricated by a method consistent with the thin film to perform this antibacterial characterization. The Cu0 and Cu1 almost formed no anti-microbial zone, and this may be attributed to the insufficiency of the doped Cu. With the increase of the Cu doped in the TiO_2 films, the anti-microbial zone formed and became larger. (Anti-microbial zone size: Cu4 > Cu3 > Cu2 > Cu1). Copper ions—which are positively charged, are easy to bind with negatively charged bacterial protein—further combine with sulfhydryl groups (-SH) of protein causing inactivation of the active enzyme, which leads to bacterium death [49]. The results above proved that the Cu doped TiO_2 thin film possessed antibacterial properties, which was positively correlated with the amounts of doped Cu; more doped Cu contributed to better antibacterial properties. Therefore, Cu4 possessed the best antibacterial function in this work.

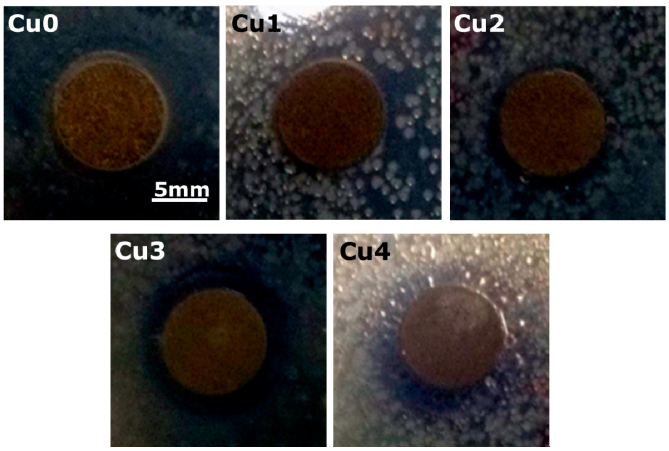

Figure 11. Antibacterial experiment of *E. coli* on the Cu0, Cu1, Cu2, Cu3 and Cu4 surfaces after 24 h of incubation.

4. Conclusions

TiO_2 films were widely applied on blood contact biomaterials for their excellent blood compatibility and mechanical behavior. In this work, different concentrations of Cu ion were doped in the TiO_2 film by a sol-gel method and dip coating process to enhance their biocompatibility. The SMC culture result demonstrated that the Cu-doped TiO_2 films could inhibit SMC attachment, proliferation and migration by inducing SNAP to release NO. The macrophages' culture result showed that the Cu-doped TiO_2 films could inhibit macrophages' attachment and activation. The anti-bacterial test proved that the Cu-doped TiO_2 films could significantly inhibit the growth of bacteria. All the properties above were positively correlated with the amounts of the doped Cu. This Cu-doped TiO_2 film was potentially anticipated and applied for the cardiovascular implanted devices.

Acknowledgments

This work was funded by the Key Basic Research Project (No. 2011CB606204), the National Natural Science Foundation of China (No.31570963), China Postdoctoral Science Foundation (2014M562333), Postdoctoral Funds of Southwest jiaotong University (X1101512370435 and YH1101012371444), and the Fundamental Research Funds for the Central Universities (NO.SWJTU11ZT11 and SWJTU11CX054).

Author Contributions

Linhua Li, Ying Xu, Zhi Zhou, Jiang Chen, Ping Yang and Nan Huang contributed to the research idea and the framework of this study. Jing'an Li contributed to the improved research method of this study. Linhua Li and Jing'an Li contributed to the article preparation of this study. The other authors contributed equal help to the study.

Conflicts of Interest

The authors declare no conflict of interest.

References

1. Williams, D.F. On the mechanisms of biocompatibility. *Biomaterials* **2008**, *29*, 2941–2953.
2. Ratner, B.D. New ideas in biomaterials science—A path to engineered biomaterials. *J. Biomed. Mater. Res*. **1993**, *27*, 837–850.
3. Serruys, W.P.; Silber, S.; Garg, S.; van Geuns, R.J.; Richardt, G.; Buszman, E.P. Comparison of Zotarolimus-Eluting and Everolimus-Eluting Coronary Stents. *N. Engl. J. Med*. **2010**, *363*, 136–146.
4. Jukema, W.J.; Ahmed, A.N.T.; Verschuren, J.W.J.; Quax, H.A.P. Restenosis after PCI. Part 2: Prevention and therapy. *Nat. Rev. Cardiol.* **2012**, *9*, 79–90.
5. May, E.A. Antiplatelet therapy after coronary stenting: For how long? *Lancet* **2013**, *382*, 1684–1685.
6. Chia, S.; Megson, L.I.; Ludlam, A.C.; Fox, A.K; Newby, E.D. Preserved endothelial vasomotion and fibrinolytic function in patients with acute stent thrombosis or in-stent restenosis. *Thromb. Res.* **2003**, *111*, 343–349.

7. Cushman, M.; Cornell, A.; Folsom, R.A.; Wang, L.; Tsai, Y.M.; Polak, J.; Tang, Z.H. Associations of the β-fibrinogen Hae III and factor VIII Val34Leu gene variants with venous thrombosis. *Thromb. Res.* **2007**, *121*, 339–345.
8. Ogita, M.; Miyauchi, K.; Jiang, M.; Kasai, T.; Tsuboi, S.; Naito, R.; Konishi, H.; Dohi, T.; Yokoyama, T.; Okazaki, S.; *et al.* Circulating soluble LR11, a novel marker of smooth muscle cell proliferation, is enhanced after coronary stenting in response to vascular injury. *Atherosclerosis* **2014**, *237*, 374–378.
9. Pfisterer, M.; Brunner-La, R.H.P.; Buser, P.T.; Rickenbacher, P.; Hunziker, P.; Mueller, C. Late clinical events after clopidogrel discontinuation may limit the benefit of drug-eluting stents: An observational study of drug-eluting *versus* bare-metal stents. *J. Am. Coll. Cardiol*. **2006**, *48*, 2584–2591.
10. Eisenstein, E.L.; Anstrom, K.J.; Kong, D.F.; Shaw, L.K.; Tuttle, R.H.; Mark, D.B. Clopidogrel use and long-term clinical outcomes after drug-eluting stent implantation. *JAMA J. Am. Med. Assoc*. **2007**, *297*, 159–168.
11. Scott, N.A. Restenosis following implantation of bare metal coronary stents: Pathophysiology and pathways involved in the vascular response to injury. *Adv. Drug Deliv. Rev*. **2006**, *58*, 358–376.
12. Woods, T.C.; Marks, A.R. Drug-eluting stents. *Annu. Rev. Med*. **2004**, *55*, 169–178.
13. McDonald, A.R.; Halliday, A.C.; Miller, M.A.; Diver, A.L.; Dakin, S.R.; Montgomery, J.; McBride, W.M.; Kennedy, S.; McClure, D.J.; Robertson, E.K.; *et al.* Reducing In-Stent Restenosis: Therapeutic Manipulation of miRNA in Vascular Remodeling and Inflammation. *J. Am. Coll. Cardiol*. **2015**, *65*, 2314–2327.
14. Hoffman, M.; Baruch, R.; Kaplan, E.; Mittelman, M.; Aviram, G.; Siegman-Igra, Y. Coronary stent bacterial infection with multiple organ septic emboli. *Eur. J. Intern. Med*. **2005**, *16*, 123–125.
15. Cai, Z.H.; Shen, L.H.; He, B. Moving with and beyond CANTOS: How to put out the fire of inflammation in atherosclerosis? *Int. J. Cardiol*. **2015**, *195*, 45–47.
16. Vitiello, L.; Spoletini, I.; Gorini, S.; Pontecorvo, L.; Ferrari, D.; Ferraro, E.; Stabile, E.; Caprio, M.; Sala, A. Microvascular inflammation in atherosclerosis. *IJC Metab. Endocr*. **2014**, *3*, 1–7.
17. Pearson, T.A.; Mensah, G.A.; Alexander, R.W.; Anderson, J.L.; Cannon, R.O.; Criqui, M. Markers of inflammation and cardiovascular disease application to clinical and public health practice: A statement for healthcare professionals from the centers for disease control and prevention and the American Heart Association. *Circulation* **2003**, *107*, 499–511.
18. Mombelli, A. Microbiology and antimicrobial therapy of peri-implantitis. *Periodontology* **2002**, *28*, 177–189.
19. Javed, F.; AlGhamdi, A.S.T.; Ahmed, A.; Mikami, T.; Ahmed, H.B.; Tenenbaum, H.C. Clinical efficacy of antibiotics in the treatment of peri-implantitis. *Int. Dent. J*. **2013**, *63*, 169–176.
20. Diebold, U. The surface science of titanium dioxide. *Surf. Sci. Rep*. **2003**, *48*, 53–229.
21. Li, J.A.; Yang, P.; Zhang, K.; Ren, H.L.; Huang, N. Preparation of SiO_2/TiO_2 and TiO_2/TiO_2 micropattern and their effects on platelet adhesion and endothelial cell regulation. *Nucl. Instrum. Methods Phys. Res. Sec. B Beam Interact. Mater. Atoms* **2013**, *307*, 575–579.
22. Xiang, L.J.; Li, C.H.; Yang, P.; Li, J.A.; Huang, N. Fabrication of micro-patterned titanium dioxide nanotubes thin film and its biocompatibility. *J. Eng*. **2014**, doi:10.1049/joe.2014.0274.

23. Zhou, Z.; Chen, J.; Xiang, L.J.; Xu, Y.; Yang, P.; Li, J.A.; Wu, J.J.; Huang, N. Fabrication of 3D TiO_2 micromesh on silicon surface and its effects on platelet adhesion. *Mater. Lett*. **2014**, *132*, 149–152.
24. Xiang, L.J.; Li, J.A.; He, Z.K.; Wu, J.J.; Yang, P.; Huang, N. Design and construction of TiO_2 nanotubes in microarray using two-step anodic oxidation for application of cardiovascular implanted devices. *Micro Nano Lett*. **2015**, *10*, 287–291.
25. Akhavan, O.; Ghaderi, E. Photocatalytic Reduction of Graphene Oxide Nanosheets on TiO_2 Thin Film for Photoinactivation of Bacteria in Solar Light Irradiation. *J. Phys. Chem. C* **2009**, *113*, 20214–20220.
26. Akhavan, O.; Ghaderi, E. Flash Photo Stimulation of Human Neural Stem Cells on Graphene/TiO_2 Heterojunction for Differentiation into Neurons. *Nanoscale* **2013**, *5*, 10316–10326.
27. Akhavan, O. Lasting antibacterial activities of Ag-TiO_2/Ag/a-TiO_2 nanocomposite thin film photocatalysts under solar light irradiation. *J. Colloid Interface Sci*. **2009**, *336*, 117–124.
28. Cui, B.; Huang, L.; Fang, Y.Q.; Guo, R.W.; Yin, Y.G.; Zhao, X.H. Transplantation of endothelial progenitor cells overexpressing endothelial nitric oxide synthase enhances inhibition of neointimal hyperplasia and restores endothelium-dependent vasodilatation. *Microvasc. Res.* **2011**, *81*, 143–150.
29. Yamawaki, H.; Kameshima, S.; Usui, T.; Okada, M.; Hara, Y. A novel adipocytokine, chemerin exerts anti-inflammatory roles in human vascular endothelial cells. *Biochem. Biophys. Res. Commun*. **2012**, *423*, 152–157.
30. Delledonne, M.; Xia, Y.; Dixon, R.A.; Lamb, C. Nitric oxide functions as a signal in plant disease resistance. *Nature* **1998**, *394*, 585–588.
31. Broughton, G.; Janis, J.E.; Attinger, C.E. The basic science of wound healing. *Plast. Reconstr. Surg*. **2006**, *117*, 12S–34S.
32. Rizk, M.; Witte, M.B.; Barbul, A. Nitric oxide and wound healing. *World J. Surg*. **2004**, *28*, 301–306.
33. Isenberg, J.S.; Ridnour, L.A.; Espey, M.G.; Wink, D.A.; Roberts, D.A. Nitric oxide in wound-healing. *Microsurgery* **2005**, *25*, 442–451.
34. Dicks, A.P.; Williams, D.L.H. Generation of nitric oxide from *S*-nitrosothiols using protein-bound Cu^{2+} sources. *Chem. Biol*. **1996**, *3*, 655–659.
35. Williams, D.L.H. The chemistry of *S*-nitrosothiols. *Acc. Chem. Res.* **1999**, *32*, 869–876.
36. Oh, B.K.; Kim, Y.K.; Park, K.W.; Lee, W.H.; Choi, J.W. Surface plasmon resonance immunosensor for the detection of *Salmonella typhimurium*. *Biosens. Bioelectron*. **2004**, *19*, 1497–1504.
37. Ignarro, L.J.; Balestrieri, M.L.; Napoli, C. Nutrition, physical activity, and cardiovascular disease: An update. *Cardiovasc. Res*. **2007**, *73*, 326–340.
38. Radomski, M.V.; Latham, C.A.T. *Occupational Therapy for Physical Dysfunction*; Lippincott Williams & Wilkins: Philadelphia, PA, USA, 2008.
39. Xu, Y.; Li, J.A.; Yao, L.F.; Li, L.H.; Yang, P.; Huang, N. Preparation and characterization of Cu-doped TiO_2 thin films and effects on platelet adhesion. *Surf. Coat. Technol*. **2015**, *261*, 436–441.
40. Wu, J.J.; Li, J.A.; Wu, F.; He, Z.K.; Yang, P.; Huang, N. Effect of micropatterned TiO_2 nanotubes thin film on the deposition of endothelial extracellular matrix: For the purpose of enhancing surface biocompatibility. *Biointerphases* **2015**, doi:10.1116/1.4928304.

41. Luo, R.F.; Tang, L.L.; Zhong, S.; Yang, Z.L.; Wang, J.; Weng, Y.J.; Tu, Q.F.; Jiang, C.X.; Huang, N. *In vitro* investigation of enhanced hemocompatibility and endothelial cell proliferation associated with quinone-rich polydopamine coating. *ASC Appl. Mater. Interfaces* **2013**, *5*, 1704–1714.
42. Wink, D.A.; Cook, J.A.; Kim, S.Y.; Vodovotz, Y.; Pacelli, R.; Krishna, M.C. Superoxide modulates the oxidation and nitrosation of thiols by nitric oxide-derived reactive intermediates chemical aspects involved in the balance between oxidative and nitrosative stress. *J. Biol. Chem*. **1997**, *272*, 11147–11151.
43. Li, J.A.; Zhang, K.; Xu, Y.; Chen, J.; Yang, P.; Zhao, Y.C.; Zhao, A.S.; Huang, N. A novel co-culture model of HUVECs and HUASMCs by hyaluronic acid micro-pattern on titanium surface. *J. Biomed. Mater. Res. A* **2014**, *102*, 1950–1960.
44. Li, J.A.; Zhang, K.; Yang, P.; Liao, Y.Z.; Wu, L.L.; Chen, J.L.; Zhao, A.S.; Li, G.C.; Huang, N. Research of smooth muscle cells response to fluid flow shear stress by hyaluronic acid micro-pattern on a titanium surface. *Exp. Cell Res*. **2013**, *319*, 2663–2672.
45. Li, G.C.; Yang, P.; Qin, W.; Maitz, M.F.; Zhou, S.; Huang, N. The effect of coimmobilizing heparin and fibronectin on titanium on hemocompatibility and endothelialization. *Biomaterials* **2011**, *32*, 4691–4703.
46. Che, H.L.; Bae, I.H.; Lim, S.K.; Song, T.I.; Lee, H.; Muthiah, M.; Namgung, R.; Kim, J.W.; Kim, D.G.; Ahn, Y.; *et al.* Suppression of post-angioplasty restenosis with an Akt1 siRNA-embedded coronary stent in a rabbit model. *Biomaterials* **2012**, *33*, 8548–8556.
47. Chang, H.; Ren, K.F.; Wang, J.L.; Zhang, H.; Wang, B.L.; Zheng, S.M.; Zhou, Y.Y.; Ji, J. Surface-mediated functional gene delivery: An effective strategy for enhancing competitiveness of endothelial cells over smooth muscle cells. *Biomaterials* **2013**, *34*, 3345–3354.
48. Gordon, S. Alternative activation of macrophages. *Nat. Rev. Immunol*. **2003**, *3*, 23–35.
49. Grass, G.; Rensing, C.; Solioz, M. Metallic copper as an antimicrobial surface. *Appl. Environ. Microbiol*. **2011**, *77*, 1541–1547.